

HIGH-ENERGY EMISSION FROM MAGNETARS

C. THOMPSON¹ AND A. M. BELOBORODOV^{2,3}
Astrophysical Journal, 634, 565, 2005

ABSTRACT

The recently discovered soft gamma-ray emission from the anomalous X-ray pulsar 1E 1841-045 has a luminosity $L_\gamma \sim 10^{36}$ ergs s⁻¹. This luminosity exceeds the spindown power by three orders of magnitude and must be fed by an alternative source of energy such as an ultrastrong magnetic field. A gradual release of energy in the stellar magnetosphere is expected if it is twisted and a strong electric current is induced on the closed field lines. We examine two mechanisms of γ -ray emission associated with the gradual dissipation of this current. (1) A thin surface layer of the star is heated by the downward beam of current-carrying charges, which excite Langmuir turbulence in the layer. As a result, it can reach a temperature $k_B T \sim 100$ keV and emit bremsstrahlung photons up to this characteristic energy. (2) The magnetosphere is also a source of soft γ -rays at a distance of ~ 100 km from the star, where the electron cyclotron energy is in the kilo-electron volt range. A large electric field develops in this region in response to the outward drag force felt by the current-carrying electrons from the flux of kilo-electron volt photons leaving the star. A seed positron injected in this region undergoes a runaway acceleration and upscatters X-ray photons above the threshold for pair creation. The created pairs emit a synchrotron spectrum consistent with the observed 20-100 keV emission. This spectrum is predicted to extend to higher energies and reach a peak at ~ 1 MeV.

Subject headings: gamma rays: stars: neutron – X-rays: stars

1. INTRODUCTION

The Soft Gamma Repeaters and Anomalous X-ray Pulsars share several characteristics: persistent X-ray luminosities in the range $10^{34} - 10^{36}$ erg/s; spin periods between 5 and 12 s; characteristic ages $P/\dot{P} \sim 10^3 - 10^5$ yrs; the release of short (~ 0.1 s) and spectrally hard X-ray bursts; and an inferred magnetic field of $10^{14} - 10^{15}$ G. (See Woods & Thompson 2004 for a review.) The persistent X-ray emission of these “magnetars” has, until recently, been measured in the 1-10 keV band. Within that band, it can typically be modeled by a superposition of a thermal (black body) component ($k_B T_{\text{bb}} \sim 0.4$ keV) and a power law with a photon index in the range -4 to -2 . The hardness of the power law correlates with the overall activity in outbursts, and with the spindown torque (Marsden & White 2001).

Only recently has there been a convincing measurement of the persistent emission of a magnetar above 20 keV (Kuiper, Hermsen, & Mendez 2004). RXTE and Integral revealed a hard, rising energy spectrum between ~ 20 and 100 keV in the AXP 1E 1841–045, which dominates the apparent bolometric output. We focus in this paper on the important implications of this detection for the mechanism that supplies the persistent non-thermal emission of the AXPs and SGRs.

The activity of a magnetar is ultimately powered by the decay of an ultrastrong magnetic field (Thompson & Duncan 1996). Several properties of their persistent emission – the non-thermal spectrum, and the long-lived changes in \dot{P} and pulse profile following outbursts (Woods et al. 2001; Kouveliotou et al. 1998; Woods et al. 2002) – are all consistent with a non-potential (twisted) magnetosphere (Thompson, Lyutikov, & Kulkarni 2002, hereafter TLK). A twisted internal magnetic field provides a plausible (repeating) source of magnetic helicity for the exterior of the star by shearing the crust.

Magnetars are slowly rotating and their light cylinders have

large radii, $R_{\text{lc}} \equiv c/\Omega \sim 3 \times 10^{10}$ cm (about 30,000 times the neutron star radius, $R_{\text{NS}} \sim 10^6$ cm). As in radio pulsars, the rotation of the star induces a net magnetospheric charge density $\rho_{\text{co}} = -\Omega \cdot \mathbf{B}/2\pi c$ (Goldreich & Julian 1969). This drives a current flowing on the open magnetic lines, which extend from a small part of the stellar surface out to the distant light cylinder. The currents induced by a twisting motion of the crust are much stronger, and may flow everywhere inside the magnetosphere.

We focus on the region well inside the light cylinder, and make use of a simple model (TLK) to investigate the dissipative properties of such currents. The strength of the magnetic field is characterized by the surface polar field B_{pole} . The shape of the field lines depends on a single parameter: the angle $\Delta\phi_{\text{N-S}}$ through which the field lines anchored close to the magnetic poles are twisted. The poloidal field remains close to a pure dipole as long as $\Delta\phi_{\text{N-S}} \lesssim 1$ radian. Outside the star, the current density has the form

$$\mathbf{J} = \frac{c}{4\pi} \nabla \times \mathbf{B} \simeq \frac{c\mathbf{B}}{4\pi r} \sin^2 \theta \Delta\phi_{\text{N-S}} \quad (r > R_{\text{NS}}). \quad (1)$$

The current must be driven by an induced electric field against the force of gravity; a dynamic model of the current is developed in an upcoming paper (A. M. Beloborodov & C. Thompson, in preparation). Charges of opposite signs are lifted at the two footpoints of a closed magnetic line, travel along the line, and return to the star at the opposite end. Far inside the light cylinder, the co-rotation charge density is much smaller than the absolute charge density $J/\beta_{\parallel} c$ supplied by the current,

$$\frac{\rho_{\text{co}}}{J/\beta_{\parallel} c} \sim \beta_{\parallel} \left(\frac{R_{\text{max}}}{R_{\text{lc}}} \right). \quad (2)$$

Here, $\beta_{\parallel} c$ is a characteristic particle drift speed along the field lines, and $R_{\text{max}}(r, \theta) = r/\sin^2 \theta$ is the maximum extent of a field line (when the poloidal field is nearly dipolar, $\Delta\phi_{\text{N-S}} \lesssim 1$). In

¹ Canadian Institute for Theoretical Astrophysics, 60 St. George St., Toronto, ON M5S 3H8

² Department of Physics, Columbia University

³ Astro-Space Center of Lebedev Physical Institute, Profsojuznaja 84/32, Moscow 117810, Russia

contrast with the open field lines, the plasma is nearly neutral, and each end of the circuit receives a flow of charges from the opposite end. In this situation a small polarization of the magnetospheric plasma can maintain the modest co-rotation charge density. Therefore, the formation of charge-starving gaps with strong electric fields is not necessary to maintain the closed-field current.

The stability of such a large-scale, non-potential magnetic field is closely related to Taylor's conjecture for the relaxation of dilute plasmas containing a helical magnetic field (Taylor 1986). A twisting up of the external magnetic field involves a transfer of magnetic helicity from the interior of the star to its exterior. Although small-scale irregularities will be damped rapidly by reconnection (and can manifest themselves as SGR bursts), several lines of observational evidence indicate that the global helicity decays on a much longer resistive timescale. Persistent non-thermal X-ray emission is observed from a number of AXPs and SGRs over a period of a decade or longer, accompanied by little X-ray burst activity. There is no evidence for an undetected population of low-energy seismic events which would occur independently of SGR burst activity: the cumulative energy radiated in SGR bursts diverges on the high-energy tail of the burst energy distribution (e.g. Göğüş et al. 1999). In such a situation, only toroidal field energy that is dissipated *outside* the star will be converted efficiently to energetic particles and non-thermal X-rays; field energy dissipated deep in the crust will be converted largely to heat. Dissipation (resistive) timescales as long as ~ 10 years are implied in some AXPs by the observation of persistent non-thermal X-ray emission without any concurrent burst activity.

2. ELECTRON ACCELERATION, PAIR CREATION AND SURFACE HEATING

A small electric field must be present to drive the current against the force of gravity. If the positive charges lifted at the anode end of the field line are protons (mass m_p), the characteristic energy⁴ per charge in such a “minimal-resistance” circuit is $e|\Delta\Phi| \sim (GMm_p/R_{\text{NS}})(1 - R_{\text{NS}}/R_{\text{max}}) = 200(1 - R_{\text{NS}}/R_{\text{max}})$ MeV. This energy is dissipated by plasma instabilities along the circuit, in particular when the charges return to the star and hit its surface layer. Integrating the current density J (eq. [1]) over the surface of the star, one obtains the net current I and the corresponding dissipation rate $L_{\text{diss}} \sim (I/e)(GMm_p/R_{\text{NS}})$. This is $\sim 10^{35} - 10^{36}$ ergs s^{-1} for a moderately strong twist, comparable to but not exceeding the observed X-ray luminosities of SGRs and AXPs. Potential drops $e|\Delta\Phi| \gg 200$ MeV would be inconsistent with observed luminosities and imply a short dissipation timescale, excluding long-living twists. If ions carry a significant fraction of the positive charge in the circuit, one concludes that electrostatic potentials must be present which could accelerate electrons to high Lorentz factors,

$$\gamma_e \sim \gamma_e(\mathbf{e} - \mathbf{i}) \equiv \frac{GM_{\text{NS}}m_p}{R_{\text{NS}}m_e c^2} \simeq 400. \quad (3)$$

Alternatively, the upper layers of the neutron star atmosphere could be hot enough that electron-positron pairs contribute significantly to the pressure, and therefore to the current flow above the surface of the star. In this case, most of the dissipation

along the circuit must be concentrated within the atmosphere: the gravitational binding energy of an electron or positron to the star is only ~ 100 keV. The observed high energy emission would then be a direct consequence of the mechanism that supplies charges to the magnetosphere. Indeed, the number flux of charged particles that carry the current is only $\sim 10^{-2}\epsilon_J B_{15}$ of the flux of 100 keV photons (if these photons originate at the surface of the star). Here, we have expressed the current density as $J = \epsilon_J(cB_{\text{NS}}/4\pi R_{\text{NS}})$, where $\epsilon_J = \Delta\phi_{\text{N-S}} \sin^2 \theta$ from eq. (1).

A fast magnetospheric flow of charges must deposit a significant fraction of its energy in a thin, upper layer surface layer of the atmosphere. (We assume that the surface is non-degenerate and composed of light elements (H or He) in what follows.) The downward electron beam at the anode end of the field line⁵ will be subject to a strong beam instability. The initial growth length of this instability is small compared with the vertical hydrostatic scale of the target plasma, being a multiple of the plasma scale c/ω_{pe} , where $\omega_{pe} = (4\pi n_e e^2/m_e)^{1/2}$ is the electron plasma frequency. For example, when the beam has a high Lorentz factor γ_e , the growth length is $\ell_{\text{beam}} \sim \gamma_e (n_{\text{beam}}/n_e)^{-1/3} c/\omega_{pe}$. Flattening of the electron distribution function at large (relativistic) momentum implies the deposition of a minimum of $\frac{1}{2}$ of the beam energy into plasma oscillations.

The current will also be subject to anomalous resistivity in the uppermost layer of the atmosphere. Rapid cyclotron cooling keeps the temperature of the ions well below the surface cyclotron energy of $\hbar\omega_{c,p} = \hbar eB/m_p c = 6.3 B_{15}$ keV (for protons). The ion temperature is therefore typically much smaller than the electron temperature at the base of the beam-heated layer, and strong ion-sound turbulence may be excited. The resistive heating is concentrated in the upper layers of the atmosphere, where the electron drift speed $|J|/en_e$ exceeds the ion sound speed $(T_e/m_p)^{1/2}$. Here the electrons are effectively collisionless.

We now determine the electron temperature deeper in the atmosphere, where the electrons are collisional. This corresponds to electron columns larger than $N_{\text{col}} \sim \sigma_{\text{Coulomb}}^{-1} \sim \sigma_T^{-1} (kT_e/m_e c^2)^2$, where σ_{Coulomb} is the Coulomb cross section. Because the luminosity of the beam is far below the Eddington luminosity, most of the deposited energy will be conducted downward by the electrons to a Thomson depth $\tau_T \sim 1$, where cooling is effective. The downward conductive heat flux is⁶

$$Q_{\text{cond}}^- \simeq -\frac{ck_B}{\sigma_T} \left(\frac{k_B T_e}{m_e c^2} \right)^{5/2} \frac{dT_e}{dr} < 0. \quad (4)$$

We assume that the heated plasma is hydrostatically supported by electron pressure, which gives $k_B dT_e/dr \sim gm_p$ and $Q_{\text{cond}}^- \simeq -(m_p c g / \sigma_T) (k_B T_e / m_e c^2)^{5/2}$. We balance Q_{cond}^- with the rate of surface heating,

$$Q_{\text{heat}}^+ = \frac{1}{2} \frac{J}{e} (\gamma_e m_e c^2), \quad (5)$$

where $\gamma_e m_e c^2 = e|\Delta\Phi|$ is the characteristic energy dissipated per current-carrying charge. Setting $Q_{\text{cond}}^- = -Q_{\text{heat}}^+$ gives the characteristic conduction temperature

$$k_B T_Q \simeq \left(\frac{\epsilon_J}{3} \alpha_{\text{em}} \frac{B_{\text{NS}}}{B_{\text{QED}}} \right)^{2/5} \left[\frac{\gamma_e}{\gamma_e(\mathbf{e} - \mathbf{i})} \right]^{2/5} m_e c^2$$

⁴ In comparison, the electric potentials generated by a fully charge-separated plasma of particle density $\sim J/ec$ would be much stronger, by the ratio $\sim \Delta\phi_{\text{N-S}} e B_{\text{NS}}^2 / GMm = 10^{15} \Delta\phi_{\text{N-S}} B_{15}(m/m_p)$. Note that, in this paper, we use the normalization $X = X_n \times 10^9$ for quantity X , as measured in c.g.s. units.

⁵ A downward positron beam at the cathode surface would behave similarly.

⁶ The Coulomb logarithm is about unity when all the electrons are confined to their lowest Landau state.

$$\sim 160 (\varepsilon_J B_{\text{NS},15})^{2/5} \left[\frac{\gamma_e}{\gamma_e(e-i)} \right]^{2/5} \text{ keV.} \quad (6)$$

Here $\alpha_{\text{em}} = 1/137$.

Photons emerging from deep in the star cannot cool the surface layer because they are in the extraordinary polarization mode (*E*-mode, see, e.g., Sil'antev & Iakovlev 1980). The scattering of this mode is suppressed by a factor $\sim (\omega m_e c / eB)^2$ and the mode couples weakly to the beam-heated layer. (When $B > 10^{14}$ G, the interconversion of *E*-mode to *O*-mode photons only occurs deep in the star's atmosphere, where the *O*-mode photons are effectively trapped: Lai & Ho 2003.) The layer must then cool by its own emission, and most of the energy deposited at the surface will be radiated by ordinary mode (*O*-mode) photons. The scattering and absorption opacities of this mode are comparable to those in an unmagnetized plasma. For example, the scattering depth encountered by an *O*-mode photon is $\tau_O \simeq \tau_T \sin^2 \theta_{kB}$, which is $\tau_O \simeq \tau_T$ after averaging over angles.

We have calculated the free-free emission from this beam-heated atmosphere at depths greater than $\tau_T \sim \sigma_T N_{\text{col}} \sim 10^{-1}$, given the downward heat flux estimated above. The free-free emissivity $\varepsilon_{\text{ff}} \simeq (2/\pi)^{3/2} \alpha_{\text{em}} (k_B T_e / m_e c^2)^{1/2} n_e^2 \sigma_T m_e c^3$ is small at the top of the collisional portion of atmosphere, as is the Compton parameter of the *O*-mode photons, $y_O = 4 \max(\tau_O, \tau_O^2) (k_B T_e / m_e c^2)$. Deeper in the atmosphere, one can estimate the temperature at which the electrons cool down by setting $\varepsilon_{\text{ff}} \Delta r = Q_{\text{cond}}^-$, where $\Delta r \simeq k_B T_e / m_p g \sim 10^3$ cm is the vertical scale height. One finds

$$k_B T_{\text{brems}} = (2\alpha_{\text{em}} \tau_T^2)^{1/3} m_e c^2 = 120 \tau_T^{2/3} \text{ keV.} \quad (7)$$

The *O*-mode emission from this hydrostatic, conducting layer has been summed numerically. The spectrum is well-approximated by thermal bremsstrahlung with a temperature $k_B T_{\text{brems}} = 80$ keV for $\varepsilon_J B_{15} [\gamma_e / \gamma_e(e-i)] = 2$ {scaling as $k_B T_{\text{brems}} \sim [\varepsilon_J B_{15} \gamma_e / \gamma_e(e-i)]^{2/5}$ }. As shown in Fig. 1, the photon index is very hard ($\simeq -1$) below an energy $\sim k_B T_{\text{brems}}$. The calculated spectrum has a slightly more extended high energy tail than the pure bremsstrahlung spectrum.

We have generalized this calculation to include the Compton heating of the radiation as it passes through upper, hotter layers, and find a nearly identical result. The equation governing the conductive heat flux now becomes

$$\frac{dQ_{\text{cond}}^-}{dr} = -\varepsilon_{\text{ff}} - \frac{4k_B [T_e(r) - \langle T_\gamma \rangle]}{m_e c^2} \sigma_T n_e c U_\gamma, \quad (8)$$

where $U_\gamma \simeq (1 + 3\tau_T)(-Q_{\text{cond}}^-)/c$ is the energy density in the bremsstrahlung radiation at Thomson depth τ_T . A bremsstrahlung source spectrum of temperature T_{brems} is modified by Compton scattering according to $(T_{\text{brems}})^{-1} dT_{\text{brems}}/dt = 4(n_e \sigma_T c) k_B (T_e - T_{\text{brems}}) / m_e c^2$. The emergent X-ray spectrum is obtained by summing the contributing from each emitting layer, after including the effects of Compton scattering by the upper, hotter layers. The downward heat flux is diminished by Compton cooling, the effects of which are incorporated into eq. (8) using a mean temperature $\langle T_\gamma \rangle = [-d \ln(U_\gamma) / dE_\gamma]^{-1}$ near the spectral peak. This mean temperature evolves according to $\langle T_\gamma \rangle^{-1} d\langle T_\gamma \rangle / d\tau_T = -4(1 + 3\tau_T) k_B (T_e - \langle T_\gamma \rangle) / m_e c^2 + \varepsilon_{\text{ff}} (T_e - \langle T_\gamma \rangle) / T_e n_e \sigma_T Q_{\text{cond}}^-$.

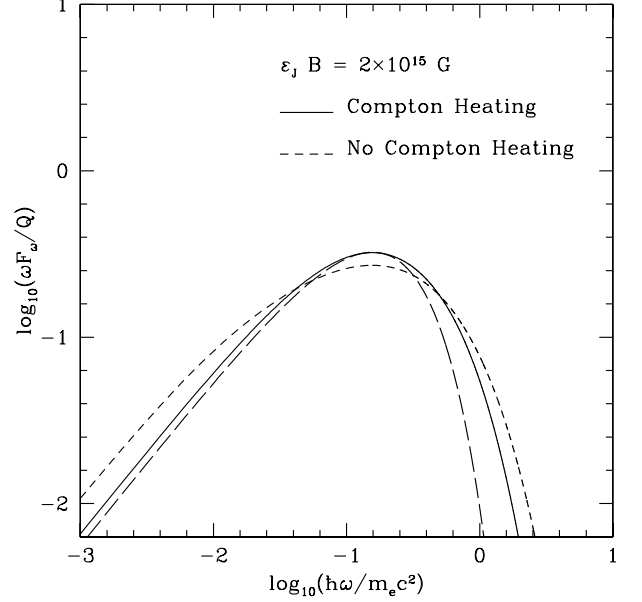


FIG. 1.— X-ray spectrum emerging from a thermal, hydrostatic, light-element atmosphere which is heated at its surface at a rate Q per unit area. The current is normalized to $\varepsilon_J B_{15} = 2$. A pure bremsstrahlung emission spectrum at $T_e = 80$ keV is shown for comparison (long-dashed curve).

It should be emphasized that hard *O*-mode photons will be able to penetrate the strong magnetic field without splitting. In this way, it is possible to hide most of the energy of the magnetospheric beam in emission above ~ 20 keV (such as is observed in 1E 1841–045; Kuiper et al. 2004).

Our model differs from the classic calculations of the X-ray emission of accreting, non-magnetic neutron star by Zel'dovich & Shakura (1969) and Shapiro & Salpeter (1975) in that i) heat is deposited directly into the electrons in a thin surface layer, and transported downward mainly by electron conduction (which is faster than advection by a factor $\sim R_{\text{NS}}/\Delta r$); and ii) the heated atmosphere is not cooled by the blackbody radiation of the star; the cooling (*O*-mode) photons are produced in the atmosphere itself at a low free-free optical depth.

The surface heating in our model results from the acceleration of a relativistic electron beam in the magnetosphere, combined with strong and localized anomalous resistivity. The acceleration is governed by electric fields which in turn are determined by the charge density distribution. The self-consistent problem of plasma dynamics in the electric circuit is addressed in a separate paper (A.M. Beloborodov & C. Thompson, in preparation). Creation of e^\pm pairs plays a crucial role in this dynamics. The presence of positrons is also important for the radiative mechanism investigated in the following section, and here we discuss briefly e^\pm production.

First, if the temperature T_e in the upper atmospheric layers reaches ~ 300 keV/ k_B , then e^+e^- pairs are created directly in the atmosphere by the conversion of thermal bremsstrahlung photons off the magnetic field. Because these photons are created in the ordinary mode, they have a threshold energy for pair creation of $\sim 2m_e c^2 / \sin \theta_{kB}$, where θ_{kB} is the angle of propagation with respect to the magnetic field. Effective pair creation at high T_e tends to regulate the upper cutoff of the persistent X-ray spectrum at ~ 300 keV, with a weak dependence on the strength of the current.

Second, a large output $L_O \sim 10^{36}$ ergs s^{-1} in > 100 keV pho-

tons from the surface of the star leads to pair creation in the magnetosphere. The X-rays are upscattered by relativistic electrons at their first Landau resonance and become gamma-rays. (In strong magnetic fields, curvature emission of gamma-rays requires much higher energies, $\gamma_e \sim 10^7$, than does resonant upscattering; e.g. Hibschan & Arons 2001.) The resonance condition is $\hbar\omega'_X \simeq (B/B_{\text{QED}})m_e c^2$ for a photon of frequency ω'_X that moves nearly parallel to the magnetic field in the rest frame of the scattering charge. (The resonance condition remains the same in super-QED magnetic fields due to the effect of the electron recoil.) Thus, the electron Lorentz factor required to resonantly upscatter an X-ray photon of frequency ω_X is

$$\gamma_e(\text{res}) \simeq 10^2 B_{15} \left(\frac{\hbar\omega_X}{100\text{keV}} \right)^{-1}. \quad (9)$$

When the magnetic field is $\sim 10B_{\text{QED}}$ or stronger, the photon emitted by the excited electron will either directly convert to an electron-positron pair (if it is emitted in the O-mode), or create a pair after undergoing the QED process of splitting (if emitted in the E-mode).

3. EFFECTS OF CYCLOTRON SCATTERING AT ~ 100 KM

The 2-10 keV X-ray output of the SGRs and AXPs is high enough that current-carrying electrons feel a strong drag force through their cyclotron resonance. At a distance from the star (50–200 km) where the resonance is in the keV range, this radiative force is much stronger than the force of gravity (TLK). In the presence of a persistent electric current, negative charges (electrons) must return to the star in one magnetic hemisphere. The force parallel to the magnetic field must therefore be compensated by an electric force,

$$F_{\text{rad}\parallel} = eE_{\parallel}. \quad (10)$$

To calculate the radiative force, we approximate the X-ray photon field as being radial at ~ 100 km. The angle θ_{kB} between an electron and incident photon is $\cos\theta_{kB} = \hat{B} \cdot \hat{r} \simeq 2\cos\theta/\sqrt{1+3\cos^2\theta}$. Here θ is the magnetic polar angle and we have assumed a nearly dipole geometry (a weak twist). An electron at rest absorbs (unpolarized) X-ray photons with a cross section $\sigma_{\text{res}} = (\pi^2 e^2/m_e c) \delta(\omega - \omega_{c,e})(1 + \cos^2\theta_{kB})$. Integrating through the cyclotron resonance $\omega_{c,e} = eB/m_e c$, the optical depth is $\tau_{\text{res}} \sim \alpha_{\text{em}}^{-1} (\hbar\omega_{c,e}/m_e c^2)^{-1} \sigma_T n_e r$.

The drag force is minimal when the electrons advance slowly to the star with a speed $\beta_{\parallel} \ll 1$. (They then supply an optical depth $\tau_{\text{res}} \sim \Delta\phi_{\text{N-S}}/\beta_{\parallel}$.) Integrating over frequency gives

$$F_{\text{rad}\parallel} \simeq \frac{\pi^2 e}{B} \left(\frac{\omega L_{\omega}}{4\pi r^2 c} \right)_{\omega_{c,e}} \cos\theta_{kb} (1 + \cos^2\theta_{kB}), \quad (11)$$

directed outwards. The potential accumulated along a given magnetic field line is given by $e\Delta\Phi = -\int_0^{\pi/2} eE_{\parallel}(dl/d\theta)d\theta$. It depends on the spectral distribution of the X-ray continuum emerging from closer to the star. For simplicity, we take a flat energy spectrum, $\omega L_{\omega} = \text{constant}$, and normalize the frequency to the cyclotron frequency $\omega_{c,e}(R_{\text{max}})$ at the maximum radius R_{max} of the field line in question, $R_{\text{max}}/R_{\text{NS}} = [eB_{\text{pole}}/2m_e c\omega_{c,e}(R_{\text{max}})]^{1/3}$. One finds,

$$\frac{e|\Delta\Phi|}{m_p c^2} = 0.3 \frac{(\omega L_{\omega})_{35}}{B_{\text{pole},15}^{1/3} R_{\text{NS},6}} \left[\frac{\hbar\omega_{c,e}(R_{\text{max}})}{\text{keV}} \right]^{-2/3}. \quad (12)$$

This is, in order of magnitude, $e|\Delta\Phi| \sim \sigma_{\text{res}}(\omega L_{\omega})/4\pi cr \sim \tau_{\text{res}}(\omega L_{\omega})/4\pi n_e r^2 c$. Notice that the electrostatic potential is proportional to the X-ray luminosity, and depends weakly on B_{pole} .

3.1. Runaway Positrons and Synchrotron Emission

A strong electrostatic potential, with a depth of hundreds of MeV, develops at a radius of ~ 100 km in the current-carrying magnetosphere of a magnetar. This has dramatic and observable consequences for the gamma-ray emission – if at least a modest fraction of the outgoing positive charges are positrons.

In the absence of radiation drag, positrons would quickly become relativistic in the electrostatic potential (12). Drag at the cyclotron resonance is ineffective if the resonance sits at or below the ~ 1 keV blackbody peak of the surface X-ray emission. To see this, note that the number density of resonant photons, of energy $\hbar\omega_{\text{res}} \sim (1 \text{ keV})\gamma_{e^+}^{-1}$, scales as $n_{\gamma}(\omega_{\text{res}}) \sim \omega_{\text{res}}^2 \sim \gamma_{e^+}^{-2}$. The drag force therefore decreases as $\gamma_{e^+}^2 (\hbar\omega_{\text{res}}) n_{\gamma}(\omega_{\text{res}}) \propto \gamma_{e^+}^{-1}$, and resonant scattering of the low-energy photons does not prevent a runaway acceleration.

The accelerated positrons will not, however, gain the full electrostatic potential because their momentum is limited by *non-resonant* inverse-Compton scattering. The optical depth for a positron to scatter a thermal X-ray photon is

$$\frac{\sigma_T L_{\omega}}{4\pi r_{\text{res}} \hbar c} = 6.2 \left(\frac{\omega L_{\omega}}{10^{35} \text{ ergs s}^{-1}} \right) \left(\frac{\hbar\omega}{\text{keV}} \right)^{-2/3} B_{\text{pole},15}^{-1/3}, \quad (13)$$

at the equatorial radius r_{res} where $\omega_{c,e} = \omega$. Thus, an accelerated positron will scatter keV photons with a mean free path $\lambda/r_{\text{res}} = 1/\sigma_T n_{\text{keV}} r_{\text{res}} \sim 0.16 (\omega L_{\omega})_{35}^{-1} B_{\text{pole},15}^{1/3}$ (where n_{keV} is the number density of the target X-ray photons).

The energy of the upscattered photons $\hbar\omega_{\text{IC}}$ can be estimated from a simple argument. The balance between Compton drag and electrostatic acceleration reads $\hbar\omega_{\text{IC}} \simeq eE_{\parallel} \lambda$. On the other hand, eq. (11) implies that $eE_{\parallel} = \sigma_{\text{res}} n_{\text{keV}} \hbar\omega$ with $\sigma_{\text{res}} \sim \pi^2 e^2/m_e c\omega$. This gives

$$\hbar\omega_{\text{IC}} \simeq \left(\frac{\sigma_{\text{res}}}{\sigma_T} \right) \hbar\omega = \frac{3\pi}{8\alpha_{\text{em}}} m_e c^2 \sim 100 \text{ MeV}. \quad (14)$$

A more accurate estimate takes into account the spectrum and angular distribution of the target X-ray photons. The drag force on the positrons is mainly due to an isotropized component of the X-ray flux, when the current-carrying electrons supply an optical depth $\tau_{\text{res}} \sim 1$. We assume that the input X-ray spectrum has a Rayleigh-Jeans cutoff at frequencies lower than $\omega_{\text{bb}} \sim 1 \text{ keV}/\hbar$. In parts of the magnetosphere where the resonant frequency $\omega_{c,e}$ sits below ω_{bb} , the positron reaches the equilibrium energy $\langle \gamma_{e^+} \rangle^2 \simeq (\varepsilon_{c,e}/\alpha_{\text{em}} \tau_{\text{res}}) (\hbar\omega_{c,e}/m_e c^2)^{-1}$. This is independent of the normalization of the X-ray flux, $\langle \gamma_{e^+} \rangle \sim 290 (\varepsilon_{c,e}/\tau_{\text{res}})^{1/2} (\hbar\omega_{c,e}/\text{keV})^{-1/2}$. The factor $\varepsilon_{c,e}$ is the ratio of ωL_{ω} at the frequency $\omega_{c,e}$, to the luminosity integrated up to a frequency ω_{KN} where non-resonant scattering is Klein-Nishina suppressed. One generally finds that ω_{KN} equilibrates to a value near ω_{bb} when $\tau_{\text{res}} \sim 1$. In this case $\varepsilon_{c,e} \simeq 3(\omega_{c,e}/\omega_{\text{bb}})^3$. The equilibrium energy of the positron is independent of the normalization of the X-ray flux, $\langle \gamma_{e^+} \rangle \simeq 290 (\varepsilon_{c,e}/\tau_{\text{res}})^{1/2} (\hbar\omega_{c,e}/\text{keV})^{-1/2}$. The inverse-Compton photon has an energy $\hbar\omega_{\text{IC}} \simeq \frac{4}{3} \gamma_{e^+}^2 \hbar\omega \sim 300 \tau_{\text{res}}^{-1} (\omega_{c,e}/\omega_{\text{bb}})^2 \text{ MeV}$.

The threshold energy for creating e^+e^- pairs directly off the magnetic field is $\hbar\omega_{\text{IC}} \sin\theta_{kB} \sim 0.06 (\hbar\omega_{c,e}/m_e c^2)^{-1} m_e c^2 \sim 15 \text{ MeV}$. This threshold is exceeded only in a restricted part of the magnetosphere: the accelerating potential is too weak where

$\omega_{c,e} \lesssim 0.5\omega_{\text{bb}}$. The resulting prompt synchrotron radiation peaks at $\hbar\omega_{\text{synch}} \sim 5 \times 10^{-3}\hbar\omega_{\text{IC}}$. This is,

$$\hbar\omega_{\text{synch}} \sim 1.5\tau_{\text{res}}^{-1}(\omega_{c,e}/\omega_{\text{bb}})^2 \text{ MeV} \quad (15)$$

at a radius where $0.5\omega_{\text{bb}} \lesssim \omega_{c,e} \lesssim \omega_{\text{bb}}$. Below this energy, the passively cooling particles emit a hard spectrum $\omega L_{\omega} \sim \omega^{1/2}$.

The *isotropic* power in this high-energy synchrotron tail can be estimated. The positrons that are created in situ will supply the entire current – and screen the accelerating electric field – when their density n_{e^+} satisfies $n_{e^+}\sigma_{\text{res}}r \sim \Delta\phi_{\text{N-S}}$. Here σ_{res} is the cross-section for scattering by a non-relativistic charge, and $\Delta\phi_{\text{N-S}}$ is the net twist angle of the field lines that extend to ~ 100 km. The corresponding power in the high-energy component is $L_{\text{synch}} \sim 4\pi r^2 n_{e^+} (e\Delta\Phi)c$. One sees, from eq. (12), that this isotropic power is at most comparable to the luminosity ωL_{ω} at ~ 1 keV,

$$\frac{L_{\text{synch}}}{(\omega L_{\omega})_{\omega_{c,e}}} \sim \sigma_{\text{res}} n_{e^+} r \lesssim \Delta\phi_{\text{N-S}}. \quad (16)$$

Thus, the output in 100 keV synchrotron photons is stronger in sources with stronger magnetospheric twists and increased \dot{P} .

The bolometric emission of the AXP 1E 1841–045 is dominated by a hard continuum which rises above 20 keV to at least ~ 100 keV (Kuiper et al. 2004). The unpulsed spectrum diverges as $\nu F_{\nu} \propto \nu^{1/2}$, and the pulsed fraction becomes close to unity at ~ 100 keV. This spectrum is suggestive of the emission of passively cooling, relativistic particles in a magnetic field whose cyclotron energy is less than ~ 10 keV. We conclude that the observed high energy emission is consistent with this model only if it is somewhat more collimated than the 2-10 keV emission (within ~ 1 steradian). (The large pulsed fraction observed at high energies is consistent with this requirement.) This inference is testable by observing other sources: if the output at 100 keV is consistently higher than in the 2-10 keV band,

we conclude that O-mode free-free emission in a heated surface layer is the most plausible mechanism.

It should be noted, in this regard, that a hard X-ray spectrum with a ~ -1.5 to -2 photon index between ~ 20 and 100 keV has recently been detected from SGR 1806-20 by Integral (Mereghetti et al. 2005). However, the 2–10 keV spectrum of this source is harder than it is in the case of 1E 1841–045, and it is possible that this is a single power-law component that masks a yet harder bremsstrahlung component above 100 keV. More generally, the hardness of the 2–10 keV spectrum is observed to be correlated with overall burst activity and with spindown rate in magnetar sources (Marsden & White 2001). In particular, during the activity of 1E 2259+586, the 2–10 keV hardness was observed to vary smoothly over the full range of values detected in the AXP sources (Woods et al. 2004). This pattern of spectral behavior points to second-order Fermi acceleration of the keV black body photons from the surface of the star, and can be effected by multiple resonant cyclotron scattering by magnetospheric electrons (TLK). We examine the implications of magnetospheric beam instabilities for the formation of the 2–10 keV spectrum elsewhere.

In conclusion, we have described two simple mechanisms for producing a rising energy spectrum near 100 keV in the persistent emission of the AXP 1E 1841–045. This is one of several magnetar sources which show a hard 2–10 keV spectrum, but otherwise little or no evidence for X-ray burst activity. The detection therefore provides strong evidence for a persistent electric current that is many orders of magnitude larger than the current which powers the spindown of these peculiar neutron stars.

CT is supported by the NSERC of Canada. AMB thanks CITA for its hospitality when part of this work was done, and acknowledges support by the Alfred P. Sloan Foundation.

REFERENCES

- Gögüş, E., et al. 1999, ApJ, 526, L93
 Goldreich, P. & Julian, W. H. 1969, ApJ, 157, 869
 Hibschan, J. A. & Arons, J. 2001, ApJ, 560, 871
 Kouveliotou, C., et al. 1998, Nature, 393, 235
 Kuiper, L., Hermsen, W., & Mendez M. 2004, ApJ, in press (astro-ph/0404582)
 Lai, D. & Ho, W. C. 2003, Physical Review Letters, 91, 071101
 Marsden, D. & White, N. E. 2001, ApJ, 551, L155
 Mereghetti, S., Götz, D., Mirabel, I. F., & Hurley, K. 2005, A&A, 433, L9
 Shapiro, S. L. & Salpeter, E. E. 1975, ApJ, 198, 671
 Silantev, N. A. & Iakovlev, D. G. 1980, Ap&SS, 71, 45
 Taylor, J. B. 1986, Rev. Mod. Phys., 58, 741
 Thompson, C. & Duncan, R.C. 1996, ApJ, 473, 322
 Thompson, C., Lyutikov, M., & Kulkarni, S., 2002 ApJ, 574, 332 (TLK)
 Woods, P. M., et al. 2001, ApJ, 552, 748
 Woods, P. M., et al. 2002, ApJ, 576, 381.
 Woods, P. M., et al. 2004, ApJ, 605, 378
 Woods, P. M. & Thompson C. 2004, to appear in “Compact Stellar X-ray Sources”, eds. W.H.G. Lewin and M. van der Klis, Cambridge University Press (astro-ph/0406133).
 Zel’Dovich, Y. B. & Shakura, N. I. 1969, Soviet Astronomy, 13, 175